Open- and Short-Circuit Terminated Series Stubs in Finite-Width Coplanar Waveguide on Silicon

George E. Ponchak, *Member, IEEE*, and Linda P. B. Katehi, *Fellow, IEEE*

***Abstract*— Open- and short-circuit terminated series stubs in finite-width coplanar waveguide (FCPW) fabricated on high-resistivity Si are experimentally characterized over the frequency range of 2–40 GHz. In coplanar waveguide (CPW), these stubs are typically placed in the center conductor, but in FCPW, the stubs may also be placed in the ground planes resulting in novel circuit elements with characteristics that make the stubs useful for matching circuits and filters. Equivalent circuit models for the stubs are presented, and it is shown that when the stub is in the ground plane the resonant frequency is equal, the inductance and resistance is halved, and the capacitance is double the values of the same stub in the center conductor. Furthermore, it is shown that by varying the stub position in the ground plane, higher Q stubs can be obtained.**

***Index Terms*— Bandpass filters, bandstop filters, coplanar transmission lines, coplanar waveguides.**

I. Introduction

COPLANAR waveguide (CPW) has proven to be a useful transmission line for millimeter-wave circuits, monolithic microwave integrated circuits (MMIC's), and antenna feed networks because the top-side ground planes enable easy connection of series and shunt circuit elements without via holes. In practice, most microwave substrates are placed in a package or on a metal plate to facilitate heat removal and to provide mechanical support. Thus, a back-side ground plane is also present. It has been reported that power leaks from the CPW into the parallel plates created by the upper and lower ground planes [1], [2], resulting in box-type resonances [3], [4]. Several alternatives to avoid these resonances have been proposed: absorbing materials can be used to attenuate power at the edges of the circuit [5], multiple dielectric layers can be used to decrease the propagation constant of the parallel-plate waveguide mode which inhibits power coupling [1], via holes can be incorporated to short the upper and lower ground planes and create an effective box that has a higher resonant frequency [4], or the upper ground planes can be made narrow with respect to the parallel-plate waveguide-mode wavelength to increase the resonant frequency out of the band of interest [3].

The last alternative, called finite-width coplanar waveguide (FCPW) (see Fig. 1), is attractive since it does not require extra processing steps to implement and does not alter the planar character of the line. Although open- and short-circuit shunt stubs in FCPW have been used in the design and fabrication of filters on GaAs [6], active antennas on Teflon fiberglass substrates [7], and instantaneous frequency-measurement units on Alumina [8], there has not been a characterization of the series stubs in FCPW. In this paper, an extensive experimental characterization of FCPW short- and open-circuit series stubs, which are implemented in novel ways and fabricated on unthinned, high-resistivity Si substrates is presented, and several new and interesting results are discussed.

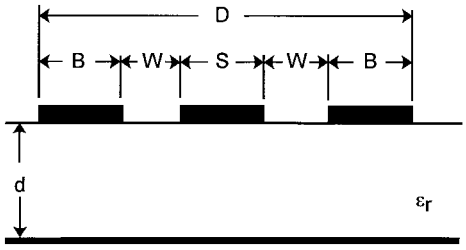

Fig. 1. Schematic of FCPW.

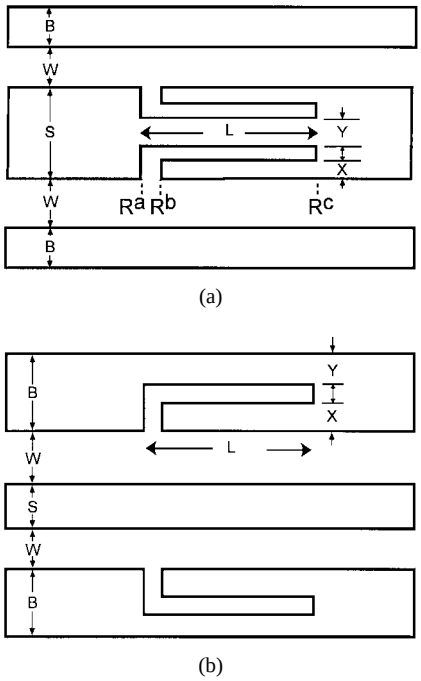

Fig. 2. Schematic of short-circuit terminated series stubs (a) in the center conductor and (b) in the ground plane.

Manuscript received October 8, 1996; revised February 28, 1997.

G. E. Ponchak is with the Electron Device Technology Branch, NASA Lewis Research Center, Cleveland, OH 44135 USA.

L. P. B. Katehi is with the Department of Electrical Engineering and Computer Science, University of Michigan, Ann Arbor, MI 48109-2122 USA.

Publisher Item Identifier S 0018-9480(97)03921-5.

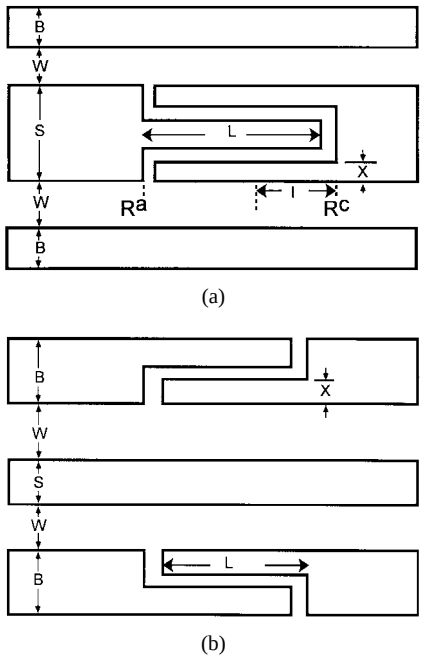

Fig. 3. Schematic of open-circuit terminated series stubs (a) in the center conductor and (b) in the ground plane.

II. FCPW Series Stub Design

CPW short- and open-circuit series stubs have been theoretically and experimentally characterized [9], [10], and have been used in filters [11] and reflective switches [12]. In each of these circuits, the stubs are implemented in the typical manner by deforming the center conductor of the CPW as shown in Figs. 2(a) and 3(a) [13]. The short-circuit series stub in the center conductor, i.e., *center short stub*, can be modeled as an equivalent transmission line [12] or as a series inductor with parasitic elements [9], [10], as shown in Fig. 4(a) and 4(b), respectively. In bandstop filters, the length of the stub is designed to be $\lambda_g/4$ at the stopband frequency, whereas the length of the stub is typically kept less than $\lambda_g/10$ when used as an inductor with the inductance determined by the length L and width Y of the center conductor between the stubs [9], [10]. The open-circuit series stub in the center conductor, i.e., *center open stub*, can be modeled as an equivalent transmission line [12] or as a series capacitor with parasitic elements [9], [11] as shown in Fig. 5(a) and 5(b), respectively. If the length of the center open stub is equal to $\lambda_g/4$, the stub has a bandpass filter characteristic, whereas if the center open stub is used as a capacitor, the length is typically kept less than $\lambda_g/10$ with the capacitance dependent on the stub length and the slot width [9], [10].

By using FCPW, it is possible to implement the same stubs in the ground planes that exist on either side of the center conductor as shown in Figs. 2(b) and 3(b), respectively, for the short-circuit series stub, i.e., *ground short stub*, and the open-circuit series stub, i.e., *ground open stub*. Note that it is impossible to implement the ground open stub in conventional CPW, and although the ground short stub can be implemented in CPW, it is not possible to control width Y of the current path in Fig. 2(b) as it is in FCPW. The characteristics of these two new stubs, with respect to the width parameter Y and the stub length L, along with a comparison of those characteristics with the characteristics of the stubs in the center conductor, is presented in this paper.

III. Measurement Technique

The circuits have been fabricated using standard MMIC fabrication techniques on double-sided polished Si wafers with a resistivity greater than 2500 Ω cm and a thickness d of 411 μm. Lift-off technology is used to define the metal lines which consist of 200 Å of Ti and 1.3 μm of Au. The back-side ground plane also consists of 200 Å of Ti and 1.3 μm of Au. All of the CPW lines presented in this paper have an S, W, and B of 50 μm, and the stubs have 10-μm slot widths (see Figs. 1–3), and 1475- and 980-μm lengths. For the stubs in the ground plane, values of $X = 10$, 20, and 30 μm are considered, while the stubs in the center conductor have $X = 10$ μm.

Measurements are made using an HP8510 network analyzer, a Cascade probe station, and GGB Industries Picoprobes. A full thru-reflect line (TRL) calibration is performed using calibration standards fabricated on the wafer with the reference planes at the ends of the stubs as shown in Figs. 2 and 3, respectively, at positions R^a and R^c. The reference impedance is determined by the characteristic impedance of the delay lines which is approximately 59 Ω for the lines used in this paper. All data presented in this paper are normalized to that impedance. Four delay lines are used in the calibration with the longest being 1.0 cm to cover the frequency range of 2–40 GHz. The TRL calibration is implemented through the program Multical [14] which utilizes all of the delay lines at each frequency point through a weighted averaging algorithm. To reduce random errors in the measurements and in the fabrication, three of each circuit are measured from different locations on the wafer and the S-parameters are averaged.

IV. Results and Discussion

Series short-circuit and the series open-circuit stubs are characterized to determine their characteristics as bandstop or bandpass filters, respectively, by measuring the resonant frequency and Q of the circuits as a function of X. In addition, the characteristics of the stubs when used as series inductors and capacitors are derived and equivalent circuits are presented to model these elements.

A. Short-Circuit Series Stub

The measured insertion loss $|S_{21}|$ for the center short stubs and the ground short stubs, is shown in Fig. 6 where it is noticed that all of the stubs have the same resonant frequency f_r, which is accurately predicted by

$$f_r = \frac{c}{4L\sqrt{\varepsilon_{\text{eff}}^{\text{cpw}}}}$$

where c is the velocity of light and $\varepsilon_{\text{eff}}^{\text{cpw}}$ is the effective permittivity of the FCPW line as determined during the TRL calibration. Therefore, the transmission-line model of the stub

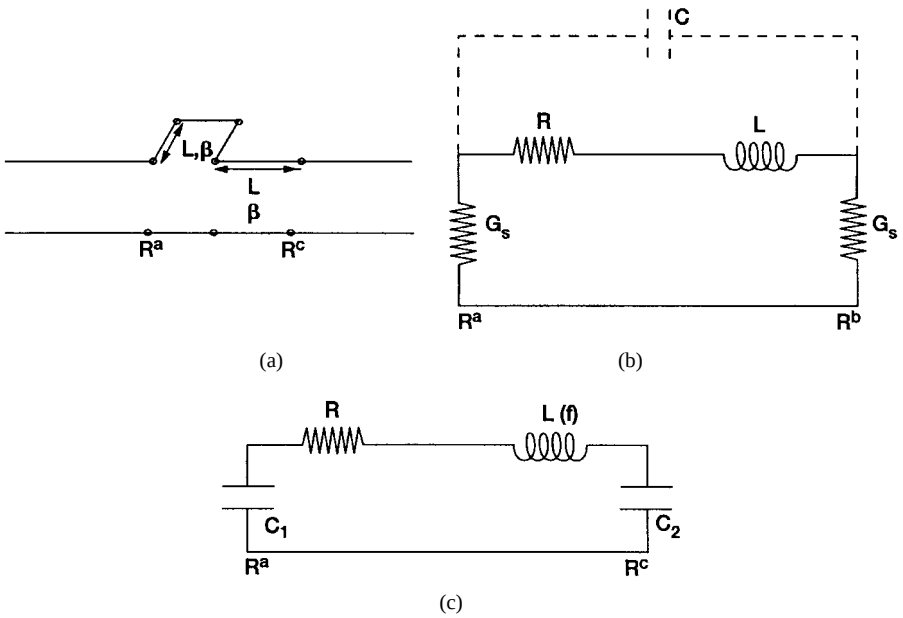

Fig. 4. Equivalent circuit of short-circuit terminated series stub. (a) Transmission-line model. (b) Symmetric circuit model with translated reference planes. (c) Asymmetric circuit model.

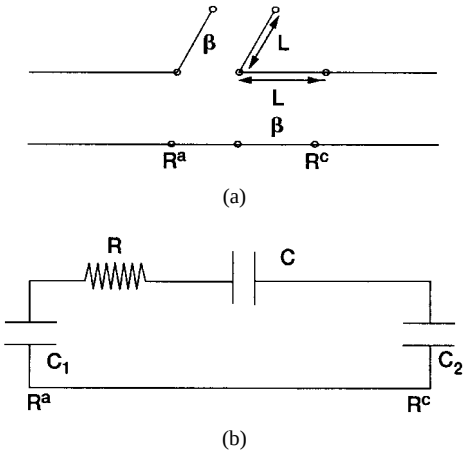

Fig. 5. Equivalent circuit of open-circuit terminated series stub. (a) Transmission-line model. (b) Asymmetric circuit model.

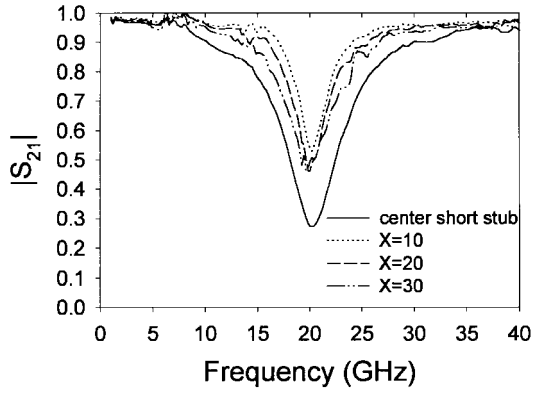

Fig. 6. Measured $|S_{21}|$ of short-circuit terminated series stubs with $L = 1475\ \mu$m.

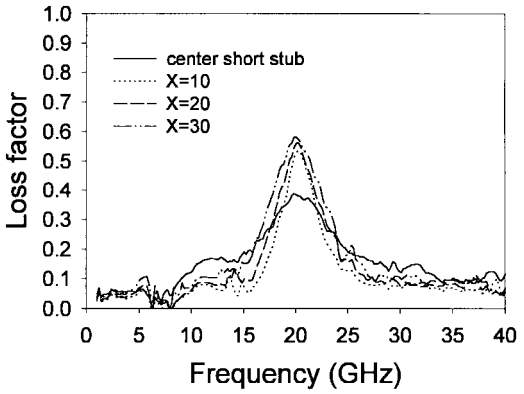

Fig. 7. Measured loss factor for short-circuit terminated series stubs with $L = 1475\ \mu$m.

as shown in Fig. 4(a) is valid regardless of the placement of the stub in the center conductor or the ground plane. The center short stub has greater stopband rejection, but it also has a broader stopband than the stubs in the ground planes. The narrowest stopband is obtained when the stub is placed in the ground plane with $X = 10$ and approaches the stub characteristics of the center short stub as X increases. From the measured S-parameters, the loss factor $1-|S_{11}|^2-|S_{12}|^2$ is calculated and plotted in Fig. 7, which shows that for $f < f_r$ and $f > f_r$, the loss factor is lower when the stubs are in the ground plane, but when $f \approx f_r$, the loss factor for the ground short stubs is greater. The reason for this will be discussed when the equivalent circuits are introduced.

To develop a low-frequency model of the stub, the reference plane R^c shown in Fig. 2 could be translated to R^b by adding $2\beta^{\mathrm{cpw}}L$ to the phase of S_{22} and $\beta^{\mathrm{cpw}}L$ to the phase of S_{12}. Fig. 8(a) and 8(b) shows the phase of the center short stub, which is typical of all the short-circuit terminated stubs before and after the reference-plane translation, respectively. Note that if the reference plane is not translated, the stub appears inductive looking into R^a through f_r; however, when looking into R^c, it appears inductive only for $f \ll f_r$. When R^c is translated to R^b, the difference in phase between S_{11} and S_{22}

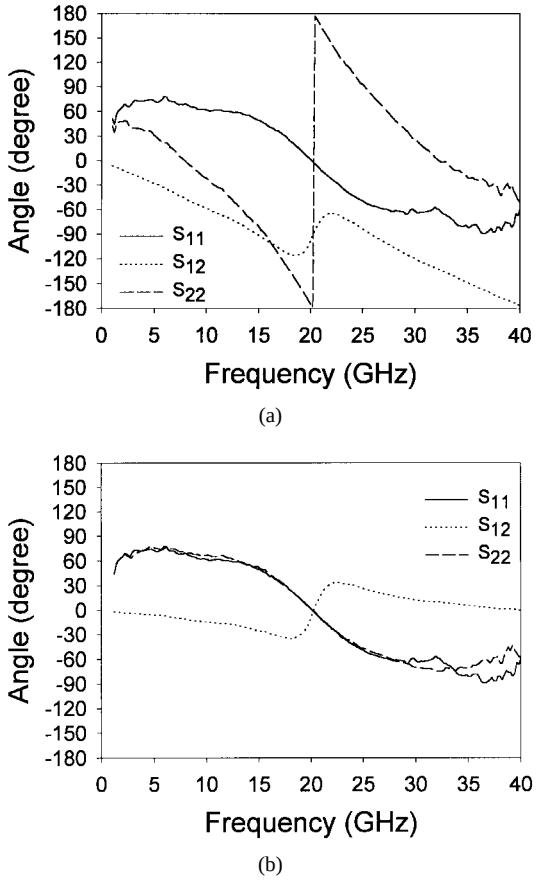

Fig. 8. Measured phase of center short stub with $L = 1475$ μm (a) before reference-plane translation and (b) after reference-plane translation.

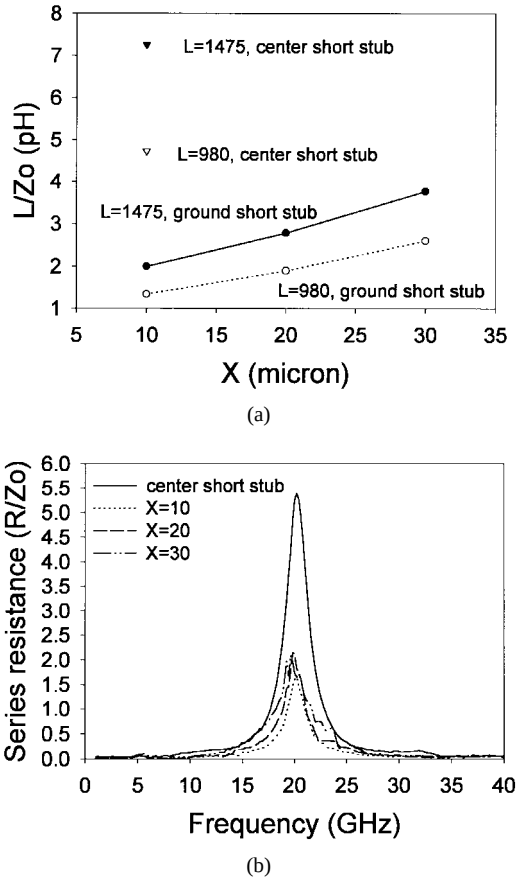

Fig. 9. Deembedded equivalent circuit model element values of short-circuit terminated series stubs modeled as shown in Fig. 4(b). (a) L. (b) R.

is less than $\pm 5°$ for $f < f_r$, and the stub appears inductive looking into both ports. R^a is not translated to maintain the proper reference planes for the limiting case of straight stubs.

Using the measured S-parameters translated to the new reference planes, an equivalent symmetric Π network is derived, and for $f < f_r/2$, the simple model shown in Fig. 4(b), adequately describes the stub with the inductance for each of the stubs shown in Fig. 9(a). For the ground short stubs, the inductance increases as X increases, or Y decreases, which agrees with the results for center short stubs [10]. Furthermore, the maximum inductance for the stubs in the ground plane is half of the inductance for the corresponding stub in the center conductor, and the inductance per-unit stub length is constant for all of the cases measured. The series resistance of the stubs over the frequency range of 2–40 GHz is shown in Fig. 9(b) and indicates that the resistance of the center short stub is approximately twice the resistance of the ground short stubs. These results imply that the impedance of the stubs in the ground plane add as parallel circuit elements and that the impedance of each of the ground short stubs is approximately equal to the impedance of the center short stub. The shunt conductance G_s is equal to zero over most of the frequency range except near f_r where G_s increased for the ground short stubs to approximately 0.05, whereas it remained nearly zero for the stub in the center conductor. Therefore, the loss factor is higher for the center short stubs due to the higher series resistance, except near the resonant frequency where the ground short stubs have higher radiation loss. The above observations are made for the 1475-μm-long stubs and are found to be valid for the 980-μm-long stubs with the exception that the radiation loss of the ground short stubs did not increase substantially at f_r, resulting in a loss factor at f_r that is independent of the stub placement. To extend the equivalent circuit model through f_r, a capacitance can be added in parallel with the series *RL* circuit with a value that yields the correct resonant frequency.

In the above discussions, the equivalent circuit represents the extra impedance created by the stubs since the reference planes have been translated, but in some circuit applications, it is desirable to have an equivalent circuit model with the reference planes at R^a and R^c. Fig. 4(c) shows the equivalent circuit model for this case, which is valid for $f < f_r/2$. Although the series resistance and the two shunt capacitors are found to be approximately frequency independent for $f \ll f_r$, the series inductance decreased linearly from its zero frequency value with increasing frequency. Fig. 10 shows the slope of the inductance, the low-frequency inductance value, the series resistance, and the shunt capacitance values where it is seen that the inductance of the ground short stub is no longer half of the value of the center short stub and the shunt capacitances C_1 and C_2 both approach the corresponding capacitance values for the center short stub, except that C_1

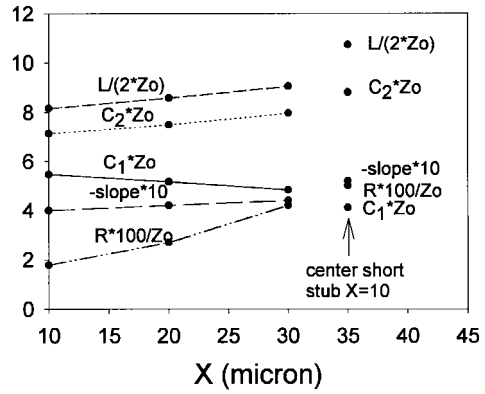

Fig. 10. De-embedded equivalent circuit model element values of short-circuit terminated series stubs with $L = 1475$ μm modeled as shown in Fig. 4(c) where L is in picohenries, C is in picofarades, and R is in ohms.

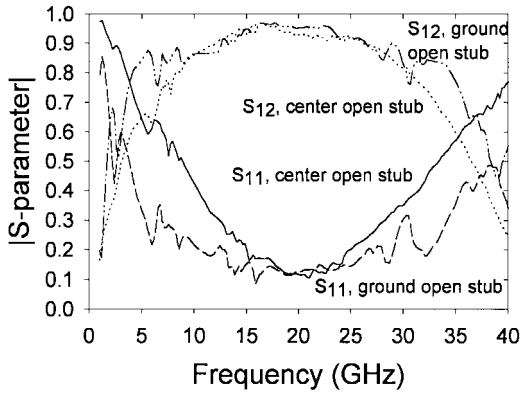

Fig. 11. Measured $|S_{12}|$ and $|S_{11}|$ of open-circuit terminated series stubs with $L = 1475$ μm.

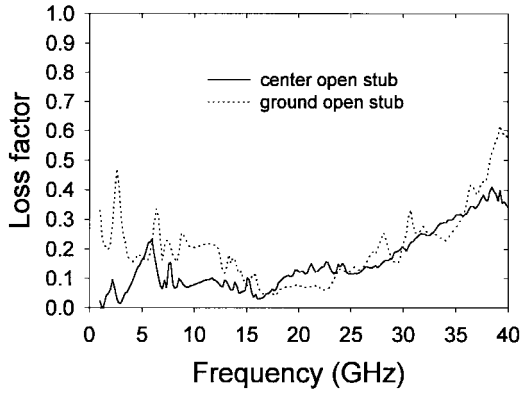

Fig. 12. Measured loss factor of open-circuit terminated series stubs with $L = 1475$ μm.

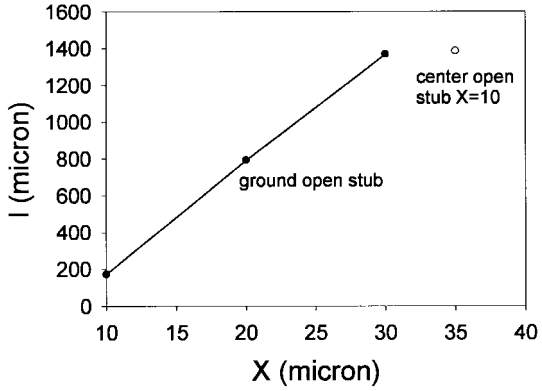

Fig. 13. Distance reference plane R^c must be translated to obtain a symmetric circuit for the open-circuit terminated series stubs with $L = 1475$ μm.

decreases in value while C_2 increases in value as X increases. It is also interesting to observe that the frequency dependance of the inductance of the ground short stubs is not half that of the center short stubs and that the frequency dependance increases as X increases. As a result, the two ground stubs do not look like two parallel stubs.

The results indicate that the ground short stubs have a lower equivalent series inductance and a lower series resistance than the center short stubs, which results in the stubs having a Q that is equivalent for both types of stubs when Y is equal, and a higher Q for ground short stubs with a larger Y. Furthermore, the resonant frequency of ground short stubs and center short stubs is equivalent. It is also determined that the inductance of the ground short stubs could be varied by a factor of two by varying the parameter X while maintaining a minimum line width of 10 μm. This is not possible for the center short stubs and should prove useful in circuit design where fabrication tolerances must be maintained for high yield.

B. Open-Circuit Series Stub

The measured insertion loss $|S_{21}|$ and return loss $|S_{11}|$ for all of the ground open stubs is identical, and thus, only one from the set is shown in Fig. 11 along with the characteristics of the center open stub. It is shown that all of the stubs have the same resonant frequency, f_r, which implies that the general model of the stub illustrated in Fig. 5(a) is valid, and the bandwidth of the passband is larger for the ground open stubs compared to the center open stubs. As shown in Fig. 12, the loss factor for the center open stubs is lower than for the ground open stubs for $f < f_r$; they both have a minimum at f_r, while for $f \geq f_r$, the loss factors of the different stubs is nearly equal.

To develop an equivalent circuit of the open-circuit stubs, it is first necessary to determine the reference planes. It has been reported that the reference plane R^c could be translated toward the center of the stub to develop a symmetric equivalent circuit with the amount of reference-plane translation dependent on the stub length [11]. For the stubs measured in this paper, R^c could be translated toward the center of the stub to form a symmetric model, but the amount of reference-plane translation is further dependent on the stub position as shown in Fig. 13. It is seen that the ground open stub with $X = 10$ can be approximated by a symmetric circuit, and as X increases, the asymmetry of the junction increases until it equals the asymmetry of the center open stub.

Since a uniform reference-plane translation is not possible for the open stubs, the utility of forming a symmetric equivalent circuit is not as evident, and therefore, the measured S-parameters are used to derive an equivalent asymmetric Π network, as shown in Fig. 5(b). The Y-parameters of the center open stub, which are typical of all the open stubs, are shown in

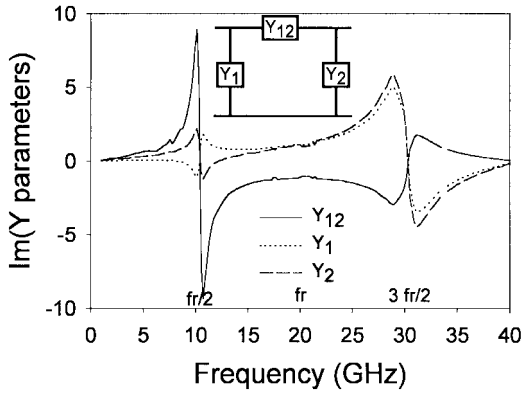

Fig. 14. Y-parameters of open-circuit terminated series stubs with $L = 1475\ \mu$m.

Fig. 14. The series reactance is capacitive only for $f < f_r/2$ and $f > 3f_r/2$ and, therefore, an equivalent transmission-line model for this structure would require an additional series stub of length $2L$ in series with the stub shown in Fig. 5(a). It is believed that this longer stub is due to the physical length of the entire stub between the two CPW slots or between the outer two edges of the center open stubs and ground open stubs, respectively.

The shunt capacitances C_1 and C_2 of the ground open stubs converge toward the capacitance values of the center open stubs from opposite directions in the same way as those discussed above for the short-circuit terminated stubs, and that C_1 and C_2 are independent of frequency. The series resistance of the ground open stubs R has a slight decrease with frequency, while R of the center open stub is independent of frequency. The series capacitance of the open-circuit terminated stubs is frequency dependant with a positive nonlinear slope. Although quantitative comparisons of the series admittance terms is difficult due to the frequency dependance, some qualitative comparisons could be made. First, the series capacitance of all the ground open stubs of the same length is equivalent, indicating the capacitance is dependent on the slot's width and length and not on the X-parameter. Second, the value of the capacitance and the frequency dependence is approximately two to four times larger for the ground open stubs compared to the center open stubs. Third, the series resistance is equivalent for all of the stubs in the ground plane of the same length, and the resistance of the ground open stubs is approximately four times the resistance of the center open stubs.

These results indicate that the ground open stubs can also be modeled as two stubs (one in each ground plane) in parallel to achieve higher capacitance values than could be achieved for the same length stub in the center conductor, which could prove useful for use in dc blocking capacitors. In addition, the ground open stubs have the same resonant frequency and broader bandwidth than the center open stubs, and since the capacitance of the ground open stubs is independent of the X-parameter, the circuit layout can accommodate manufacturing tolerances. The higher loss factor below the resonant frequency is believed to be due to leakage of energy from the open-ended slots on the outer edges of the FCPW ground planes.

V. Conclusion

An in-depth experimental characterization of short-circuit and open-circuit terminated series stubs in FCPW lines is presented. It is shown that the equivalent circuits for the stubs in the ground planes are similar to those for stubs in the center conductor, and when the stubs are in the ground plane, the series elements in the equivalent Π network can be estimated from the element values when the stub is in the center conductor by halving the resistance and inductance and doubling the capacitance. These changes in the element values predict the narrower stopband of the short-circuit terminated stubs and the broader passband of the open-circuit terminated stubs when they are placed in the ground plane. The results of this paper should enable the circuit designer to select the optimum characteristics of each stub design.

Acknowledgment

The authors would like to acknowledge the help of S. Robertson in calculating the FCPW characteristic impedance.

References

[1] R. W. Jackson, "Considerations in the use of coplanar waveguide for millimeter-wave integrated circuits," *IEEE Trans. Microwave Theory Tech.*, vol. MTT-34, pp. 1450–1456, Dec. 1986.

[2] M. Riaziat, R. Majidi-Ahy, and I.-J. Feng, "Propagation modes and dispersion characteristics of coplanar waveguide," *IEEE Trans. Microwave Theory Tech.*, vol. 38, pp. 245–251, Mar. 1990.

[3] W.-T. Lo, C.-K. C. Tzuang, S.-T. Peng, C.-C. Tien, C.-C. Chang, and J.-W. Huang, "Resonant phenomena in conductor-backed coplanar waveguides (CBCPW's)," *IEEE Trans. Microwave Theory Tech.*, vol. 41, pp. 2099–2107, Dec. 1993.

[4] M. Yu, R. Vahldieck, and J. Huang, "Comparing coax launcher and wafer probe excitation for 10-mil conductor-backed CPW with via holes and airbridges," in *IEEE Int. Microwave Symp. Dig.*, Atlanta, GA, June 14–18, 1993, pp. 705–708.

[5] K. Jones, "Suppression of spurious propagation modes in microwave wafer probes," *Microwave J.*, pp. 173–174, Nov. 1989.

[6] F. Brauchler, S. Robertson, J. East, and L. P. B. Katehi, "W-Band finite ground plane coplanar (FGC) line circuit elements," in *IEEE Int. Microwave Symp. Dig.*, San Francisco, CA, June 17–21, 1996, pp. 1845–1848.

[7] A. Nesic, S. Jovanovic, and I. Radnovic, "Integrated uniplanar oscillator-transmitter and mixer with active antennas," in *Proc. 25th European Microwave Conf.*, Bologna, Italy, Sept. 4–7, 1995, pp. 324–328.

[8] C. Sinclair, "A coplanar waveguide 6–18 GHz instantaneous frequency measurement unit for electronic warfare systems," in *IEEE Int. Microwave Symp. Dig.*, San Diego, CA, May 23–27, 1994, pp. 1767–1770.

[9] N. I. Dib, L. P. B. Katehi, G. E. Ponchak, and R. N. Simons, "Theoretical and experimental characterization of coplanar waveguide discontinuities for filter applications," *IEEE Trans. Microwave Theory Tech.*, vol. 39, pp. 873–882, May 1991.

[10] A. K. Sharma and H. Wang, "Experimental models of series and shunt elements in coplanar MMIC's," in *IEEE Int. Microwave Symp. Dig.*, Albuquerque, NM, June 1–5, 1992, pp. 1349–1352.

[11] D. F. Williams and S. E. Schwarz, "Design and performance of coplanar waveguide bandpass filters," *IEEE Trans. Microwave Theory Tech.*, vol. MTT-31, pp. 558–566, July 1983.

[12] G. E. Ponchak and R. N. Simons, "Channelized coplanar waveguide PIN-diode switches," in *Proc. 19th European Microwave Conf.*, London, U.K., Sept. 4–7, 1989, pp. 489–494.

[13] M. Houdart, "Coplanar lines: Application to broad-band microwave integrated circuits," in *Proc. 6th European Microwave Conf.*, Rome, Italy, Sept. 14–17, 1976, pp. 49–53.

[14] R. B. Marks, "A multiline method of network analyzer calibration," *IEEE Trans. Microwave Theory Tech.*, vol. 39, pp. 1205–1215, July 1991.

George E. Ponchak (S'82–M'83) received the B.E.E. degree from Cleveland State University Cleveland, OH, and the M.S.E.E. degree from Case Western Reserve University, Cleveland, OH, in 1983 and 1987, respectively. He is currently pursuing the Ph.D. degree in electrical engineering from the University of Michigan, Ann Arbor.

In July 1983, he joined the Space Communications Division, NASA Lewis Research Center, Cleveland, OH. Since then, he has been responsible for the technical management of GaAs, InP, and SiGe grants and contracts. His research interests lie in the development of microwave and millimeter-wave integrated circuits, transitions between transmission lines, coplanar waveguide, dielectric waveguide, packaging, and the reliability of microwave circuits for space applications. He has authored or co-authored over 30 papers.

Mr. Ponchak is a member of the International Microelectronics and Packaging Society.

Linda P. B. Katehi (S'81–M'84–SM'89–F'95), for a photograph and biography, see this issue, p. 938.